Available online at www.sciencedirect.com
SCIENCE DIRECT®
Coordination Chemistry Reviews 249 (2005) 313–328
COORDINATION CHEMISTRY REVIEWS
www.elsevier.com/locate/ccr

Review

Water oxidation catalyzed by dimeric μ-oxo bridged ruthenium diimine complexes

James K. Hurst*

Department of Chemistry, Washington State University, Pullman, WA 99164-4630, USA

Received 26 January 2004; accepted 24 June 2004
Available online 22 September 2004

Contents

Abstract

Dimeric μ-oxo ions such as *cis,cis*-$[(bpy)_2Ru(OH_2)]_2O^{4+}$, its congeners containing ring-substituted bipyridine ligands, and related structures have long been known to efficiently catalyze water oxidation by strong chemical oxidants and at electrode surfaces. However, despite considerable effort, the goal of identifying the underlying molecular mechanisms has not yet been realized. In this contribution issues concerning the reactivity of these catalysts are reviewed from the perspective of recent research findings, which have led to considerable clarification of the reaction pathways. Alternative postulated molecular mechanisms are also discussed within the framework of general principles governing the reactivity of group 8 polypyridyl complexes.

Keywords: Water oxidation catalysis; μ-Oxo ions; Redox reactions; Ruthenium complexes

1. Introduction and scope

Although the literature on polypyridyl and related coordination complexes is enormous, this review is narrowly focused on only one aspect of their chemistry, namely, their capacity to function as catalysts for the oxidation of water to dioxygen. Emphasis is placed upon our evolving understanding of the mechanisms of these reactions, and only those chemical aspects that bear directly upon mechanistic issues are discussed. This approach would seem to be in keeping with a volume devoted to Henry Taube, whose profound insights derived from detailed investigations of ligand substitution and redox mechanisms transformed inorganic chemistry to the extent that all subsequent research bears the indelible mark of his intellect.

* Tel.: +1 509 335 7848; fax: +1 509 335 8867.
E-mail address: hurst@wsu.edu.

0010-8545/$ – see front matter © 2004 Elsevier B.V. All rights reserved.
doi:10.1016/j.ccr.2004.06.017

There are several reasons why the catalytic oxidation of water by dimeric ruthenium μ-oxo ions is of topical interest. They afford a potentially highly tractable system to study complex noncomplementary redox reactions, in the present case in the form of a net four-electron oxidation of two water molecules that is somehow coupled to the heterolytic cleavage of four O–H bonds and formation of an O=O double bond via a series of one-electron and two-electron steps. The catalysts themselves are structurally relatively simple, synthetically versatile, and robust complexes that display numerous intermediary redox states, affording one the opportunity to probe the reaction pathways through physical and chemical identification of reaction transients. Although Ru is hardly a vitamin, these complexes may also be useful functional models for studying biological water oxidation, whose active site is an asymmetric Mn tetranuclear cluster [1] located within a protein associated with the photosystems of plants and certain bacteria. Although these clusters contain four redox metal ions, recent mechanistic models have been proposed in which it is suggested that only two of the Mn ions actually change their oxidation state in the catalytic cycle; furthermore, in these models, oxidation is accompanied by progressive deprotonation of aqua ligands, ultimately forming a manganyl (Mn=O) species whose electron-deficient oxo atom undergoes nucleophilic attack by an aqua ligand located on an adjacent metal center (Mn^{3+} or Ca^{2+}) to form a bound peroxo intermediate [2,3]. As will be evident, these same mechanistic principles appear to be operative in the more tractable homogeneous reactions catalyzed by the dimeric μ-oxo ruthenium ions. Finally, the capacity to oxidize water may be crucial to achieving long-sought technological goals such as solar photoproduction of H_2, which requires a cheap, plentiful source of electrons to close the oxidative half-cycles of coupled photoinitiated redox reactions. Insights gained from mechanistic studies on these homogeneous catalysts will almost certainly lead to development of compounds with superior catalytic properties.

2. Reactions involving monomeric complexes

It has long been known that the tris 2,2′-bipyridine and 1,10-phenanthroline complexes of group 8 trivalent ions are unstable in alkaline solutions, undergoing apparent one-electron reduction to the corresponding M(II) ions [4,5]. Early reports suggesting formation of O_3 (by olfactory detection) and accumulation of H_2O_2 in the reaction medium [6] prompted numerous laboratories to investigate the apparent mechanisms of water oxidation. Although it was initially suggested that these reactions were initiated by oxidation of OH^- to $OH^\bullet$ by an outer-sphere mechanism [7–9], e.g.

$$Fe(bpy)_3^{3+} + OH^- \rightarrow Fe(bpy)_3^{2+} + OH^\bullet \quad (1)$$

it was quickly realized from the reaction dynamics that this reaction did not occur. Specifically, measured activation enthalpies for complex ion reduction were considerably smaller than the calculated (endoergic) reaction enthalpies based upon thermodynamic potentials, necessitating the introduction of one or more intermediates in the reaction scheme [10,11]. Furthermore, addition of alcohols, halides, and other $OH^\bullet$ scavengers to the medium had no effect upon the decomposition dynamics [11–13], indicating that *free* $OH^\bullet$ was not generated. Speculations concerning the nature of the reactive intermediates included suggestions that these were: (i) pseudo-bases or covalent hydrates [14,15] formed by addition of OH^- or H_2O to ligands (Fig. 1) [10–12,16]; (ii) similar N-oxides formed by partial dissociation of the ligand and its reaction with OH^-[17]; (iii) $\{ML_3^{3+}, (OH^-)_n\}$ ion pairs that formed ligand π-stabilized $^\bullet OH(OH^-)_m$ entities which were further oxidized to form peroxides [18]; (iv) μ-oxo dimers formed by a sequence of reactions involving addition of OH^- to the primary coordination sphere, oxidation to the corresponding oxo atom, atom transfer to a ligand N atom, dissociation of the ligand N-oxide, and dimerization and oxidation of the resulting *cis*,*cis*-diaqua complex to give catalytic $[(L)_2Ru(OH_2)]_2O^{4+}$ ions [19]. Discussions of the relative merits of these proposed mechanisms can be found in the cited references; however, much of this discussion is moot because further examination of these reactions revealed that negligible O_2 was formed by decomposition of the ML_3^{3+} ions per se. In particular, upon reexamination of the spontaneous reduction of $Ru(bpy)_3^{3+}$, it was found that O_2 yields were vanishingly small [16]; copious amounts of CO_2 were evolved during the reaction and at least 10 ruthenium(II)-containing products containing modified ligands were detected, indicating the predominant source of electrons for Ru(III) reduction was the ligands themselves. Reduction of the corresponding Os(III) analogs also does not generate O_2 [17]. Furthermore, Nord and coworkers showed that yields of O_2 formed when $Fe(bpy)_3^{3+}$ and $Fe(phen)_3^{3+}$ decomposed directly correlated with the subfraction of complex ion that had undergone ligand dissociation; these ions were then suggested to catalyze the decomposition of other intermediates that contained N-oxide ligands formed by reaction of the ferric complexes with OH^- [17]. This rather complicated mechanism was supported by detection of the ligand N-oxides among the reaction products.

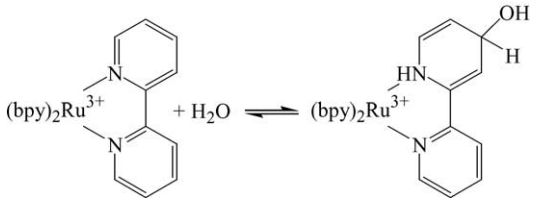

Fig. 1. Formation of a hypothetical covalent hydrate of $Ru(bpy)_3^{3+}$.

During the course of these investigations, several observations were made that may be germane to mechanisms of water oxidation catalyzed by $[(bpy)_2Ru(OH_2)]_2O^{n+}$ and its

congeners. For one, reactive intermediates possessing unusual absorption bands in the 750–800 nm region accumulate during decomposition of $Ru(bpy)_3^{3+}$ and $Fe(bpy)_3^{3+}$; their spectroscopic signatures are very similar to those obtained when a wider range of $M(bpy)_3^{2+}$ and $M(bpy)_3^{3+}$ ions are reacted with radiolytically-generated $^{\bullet}OH$ [11,17]. As with reactions of noncoordinated 2,2′-bipyridine and 1,10-phenanthroline [20,21], these latter reactions involve addition of $OH^{\bullet}$ to the heterocyclic ring, rather than electron transfer, e.g., the reverse of reaction (1). Decomposition of the isolable $Fe(bpy)_2(bpy\text{-}OH)^{2+}$ adduct(s) formed by reaction between $Fe(bpy)_3^{3+}$ and $OH^{\bullet}$ does not lead to water oxidation, however [22]. Similar oxidative addition reactions by alkyl radicals to the *tris*-Ru(III), Fe(III) and Os(III) complexes of bpy and phen have been reported by Rollick and Kochi [23]; based upon relative rate comparisons for substituted phenanthroline ligands and the ring positions of akylation, a mechanism involving *nucleophilic* addition of the radicals to the ligand was proposed. Convincing evidence has been presented by Hupp and coworkers [24,25] for nucleophilic attack upon $Ru(bpy)_3^{3+}$ and $Ru(phen)_3^{3+}$ by pyridine and bipyridine compounds and coordination complexes whose ligands contain pendant pyridinium groups; these reactions, which are facile in nonaqueous solvents, lead to formation of covalent C–N bonds at the bpy and phen 4-positions. Numerous examples exist in N-alkyl heterocyclic cations of pseudobase formation, i.e., reversible formation of covalent adducts with OH^- [26], and Gillard and his associates, in particular, have broadly interpreted the properties of coordination complexes containing N-heterocyclic compounds, including $Ru(bpy)_3^{3+}$ and $Ru(phen)_3^{3+}$ [27], in terms formation of analogous covalently hydrated species [15]. The evidence supporting this interpretation is indirect, however, and alternative explanations have been advanced [28]. In any event, there are ample precedents within the chemical literature to suggest that coordination to highly oxidized metal ions will activate bpy and phen for nucleophilic attack.

A second observation is that much higher O_2 yields have been obtained when the group 8 $M(bpy)_3^{3+}$ ions are decomposed in the presence of redox metal ions [16,29] and/or oxides [22,30–32] that can catalyze water oxidation. For example, with Co(II), near-quantitative yields of O_2 can be obtained [16], based upon the equation:

$$4M(bpy)_3^{3+} + 2H_2O \rightarrow 4M(bpy)_3^{2+} + O_2 + 4H^+ \qquad (2)$$

The form of the rate law for the catalyzed reaction is consistent with progressive one-electron oxidation of Co(II) to Co(IV), which presumably contains a bound oxo atom, i.e., "CoO^{2+}", followed by its reaction with solvent H_2O to form H_2O_2 [16,33]. Several fairly efficient photocatalytic cycles for water oxidation by electron acceptors based upon these reactions have been developed [29–31], as illustrated in the following generic scheme (Scheme 1).

In these systems, it is generally assumed that the function of the photoexcited $^*M(bpy)_3^{2+}$ ion is to transfer electrons

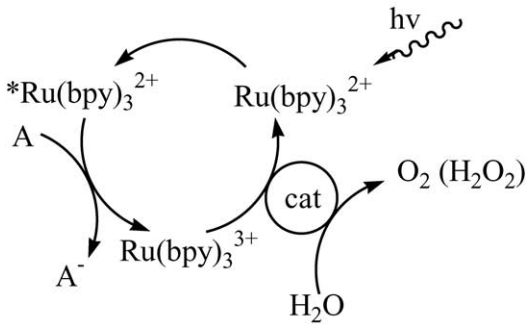

Scheme 1.

between the water oxidation catalyst and the ultimate acceptor (see, however, [34]). The presence of a second oxidizable metal ion is thought to minimize ligand decomposition on the $M(bpy)_3^{3+}$ intermediate by shortening its lifetime.

Finally, a remarkable reversal of reactivity has been reported for $Ru(bpy)_3^{3+}$ ions that were isolated within zeolite cages. Specifically, Ledney and Dutta reported that alkaline decomposition of these ions that had been synthesized within Y-zeolite supercages generated near-stoichiometric amounts of O_2 [35]. Accumulation and decay of optical bands in the 830–850 nm region were observed by diffuse reflectance spectroscopy to occur on the same timescale as $Ru(bpy)_3^{3+}$ decomposition. Cryogenic epr spectra also gave evidence of accumulation of intermediary Ru(III) species whose signals exhibited greater rhombicity than that of the parent $Ru(bpy)_3^{3+}$ ion, as might occur if one of the ligands were chemically modified. These epr signals are also similar to those of a previously isolated complex claimed to be an authentic $Ru(bpy)_2(bpy^{\bullet}OH_2)^{3+}$ covalent hydrate [14] (see, however, [28] for a skeptical view). Evidence for ligand modification in zeolite-entrapped $Ru(bpy)_3^{3+}$ ions was also obtained by resonance Raman (RR) examination of the bipyridine ring deformation modes. Deliberate addition of Co(II) to the medium resulted in rapid reduction of the complex; however, unlike the corresponding reactions in homogeneous solution, no O_2 was formed. It was argued that this difference was a consequence of immobilization of Co(III) within the zeolite lattice, preventing subsequent formation of "CoO". The inference drawn from these latter experiments was that O_2 formation by the entrapped $Ru(bpy)_3^{3+}$ was unlikely to be catalyzed by adventitious redox ions present in the zeolite. The researchers proposed a mechanism based upon formation of $Ru^{III}(bpy)_3^{n+}$ covalent hydrate and pseudo-base intermediates [35]. A critical reaction step was the further one-electron oxidation of these complexes to reactive species which could undertake net two-electron oxidations of solvent to H_2O_2. The second oxidation was supposed to occur by reaction with mobile $OH^{\bullet}$ radicals, which were formed by dissociation from a ligand radical intermediate, i.e., $Ru^{II}(bpy)_2(bpy\text{-}OH^{\bullet})^{2+}$, which in turn was formed by internal electron transfer within the pseudo-base, $Ru^{III}(bpy)_2(bpy\text{-}OH^-)^{2+}$, as part of the

overall sequence:

$$H_2O + Ru(bpy)_3^{3+} \rightarrow Ru(bpy)_2(bpy\text{-}OH_2)^{3+}$$
$$\rightarrow Ru^{III}(bpy)_2(bpy\text{-}OH^-)^{2+} + H^+$$
$$\rightarrow Ru^{II}(bpy)_2(bpy\text{-}OH^\bullet)^{2+} \rightarrow Ru(bpy)_3^{2+} + OH^\bullet \quad (3)$$

Epr signals consistent with formation of both the ligand radical complex and $OH^\bullet$ were detected in the $g \sim 2$ region of the spectra during decomposition; however, despite these reactions being very slow, accumulation of free $OH^\bullet$ seems questionable, based upon the thermodynamic constraints for the corresponding overall reaction in homogeneous solution (Eq. (1)). An earlier study made at higher cage occupancies of $Ru(bpy)_3^{3+}$ had indicated that O_2 was not formed, but that decomposition was accompanied by evolution of CO_2 [36], similar to the results reported for the uncatalyzed reactions in homogeneous solution [16]. The appearance of epr signals attributable to rhombic Ru^{III} species were also noted in that study. Presumably, the difference in reactivity arises from the proximity of $Ru(bpy)_3^{3+}$ in adjacent cages at the higher loadings [35], allowing ligand decomposition by the equivalent of bimolecular pathways to occur. If this interpretation is valid, one can conclude that a single ruthenium center is capable of catalyzing water oxidation.

3. Reactions catalyzed by the *cis,cis*-$[(bpy)_2Ru(OH_2)]_2O^{4+}$ ion

3.1. Structure and redox properties

In 1982, T.J. Meyer and coworkers reported that the ions *cis,cis*-$[(bpy)_2Ru(OH_2)]_2O^{4+}$ and *cis,cis*-$[(phen)_2Ru(OH_2)]_2O^{4+}$ were effective catalysts for water oxidation by strong oxidants [37]. These observations have been repeatedly confirmed over the past two decades by research emanating from their own laboratory [38–42] and elsewhere [43–49], and have been extended to include analogs of the type $[(L)_2Ru(OH_2)]_2O^{4+}$, where L is a substituted bipyridine ligand [50–52], as well as the structurally similar dinuclear ion, $[(tpy)Ru(OH_2)_2]_2O^{4+}$ [53], where tpy is 2,2′:6′,2″-terpyridine. Manifestations of catalysis by these μ-oxo ions have included enhanced rates of O_2 evolution by Ce^{4+} or Co^{3+} [37–42,44,46,48–50,52,53], lowered overpotentials for water oxidation at electrode surfaces [38,45,50,52], and catalysis of O_2 generation by photoresponsive electron acceptor systems (Scheme 1) [50,52]. In contrast, the monomeric analogs, *cis*-$L_2Ru(OH_2)_2^{2+}$, where L represents 6,6′-dimethyl-2,2′-bipyridine or 2,9-dimethyl-1,10-phenanthroline, have been shown to be devoid of activity despite having sufficient thermodynamic potential in their higher oxidation states to oxidize water to O_2 [44]; in these complexes, the presence of methyl groups at positions α to the nitrogen lead-in atoms sterically blocks formation of μ-oxo dimers. The activity of a dinuclear ion containing only a single coordinated water, $[(bpy)_2(py)RuORu(H_2O)(bpy)_2]^{4+}$, is also markedly reduced [54,55], as is that of a *cis-trans–cis* trimeric analog, formulated as $[(bpy)_2(H_2O)RuORu(bpy)_2ORu(OH_2)(bpy)_2]^{6+}$ [56]. These comparisons suggest that the minimal structural requirement for efficient catalysis includes the intact $(H_2O)RuORu(OH_2)$ core.

A crystal structure of the perchlorate salt of the $[(bpy)_2Ru(OH_2)]_2O^{4+}$ ion (hereafter, designated as {3,3}) revealed that bonding was nearly linear through the oxo bridge, with a Ru–O–Ru angle of 165° (Fig. 2) [38]. The μ-oxo bonds to each of the metal centers were equal in length (1.87 Å) and significantly shorter than the terminal *cis*-aqua Ru–O bonds (2.136 Å), indicating that multiple bonding existed within the Ru–O–Ru unit. Electronic delocalization across this unit has also been demonstrated by magnetic susceptibility measurements on similar μ-oxo bridged ruthenium(III) ions, e.g., *cis,cis*-$[(bpy)_2Ru(NO_2)]_2O^{2+}$ [57]. A second notable feature of the structure is the torsional angle formed by the *cis*-aqua ruthenium bonds (O1W-Ru–Ru–O1W in Fig. 2), which is ∼66°; the equilibrium internuclear distance between O atoms of the coordinated waters caused by the combined effects of this displacement from planarity and the bending of the bridge is ∼4.72 Å. In the corresponding $[(bpy)_2(OH_2)RuORu(OH)(bpy)_2]^{4+}$ perchlorate (hereafter, {3,4}), the Ru–O–Ru bridge is no longer symmetric, with Ru–O distances of 1.83 and 1.85 Å; the bridging angle is 170°, and the torsional angle is 117° [58]. Furthermore, the coordinating atoms in the equatorial positions are displaced away from the Ru–O–Ru bridge, an effect that has been attributed to increased nonbonding repulsion between the H_2O and OH^- ligands in the {3,4} ion relative to the two H_2O ligands in the {3,3} ion [58]. As a consequence of these displacements, the O–O distance between coordinated waters increases to ∼5.55 Å in the {3,4} ion. The shorter Ru–μ–O distances and displacement toward linearity in the {3,4} ion are consistent with greater π-delocalization across its bridge; however, as noted by Meyer and coworkers, the oxidation states on the individual Ru atoms must retain some localized character because other {3,4} ions that possess a symmetric set of ligands, e.g., *cis,cis*-$[(bpy)_2RuCl]_2O^{3+}$ also exhibit two different crystallographic Ru–μ–O bond lengths [58].

The Ru–O–Ru bridging angle has also been determined for the {3,3} ion in solution by RR spectroscopy [46,59]. The Ru–O–Ru unit gives rise to a very strong resonance-enhanced band in 350–400 cm^{-1} region, which is attributable to its symmetric stretching mode (ν_s) (Fig. 3) [60]. Assuming that this mode is not coupled to other molecular vibrations, the magnitude of the shift induced by isotopic substitution on the bridging O atom can be used to determine the bridging angle [60,61]. This follows because in a symmetric molecule with a linear bridge the O atom is motionless in ν_s and therefore does not contribute to the effective mass (or the vibrational frequency), whereas, if the bridge is bent, the symmetric and asymmetric stretching

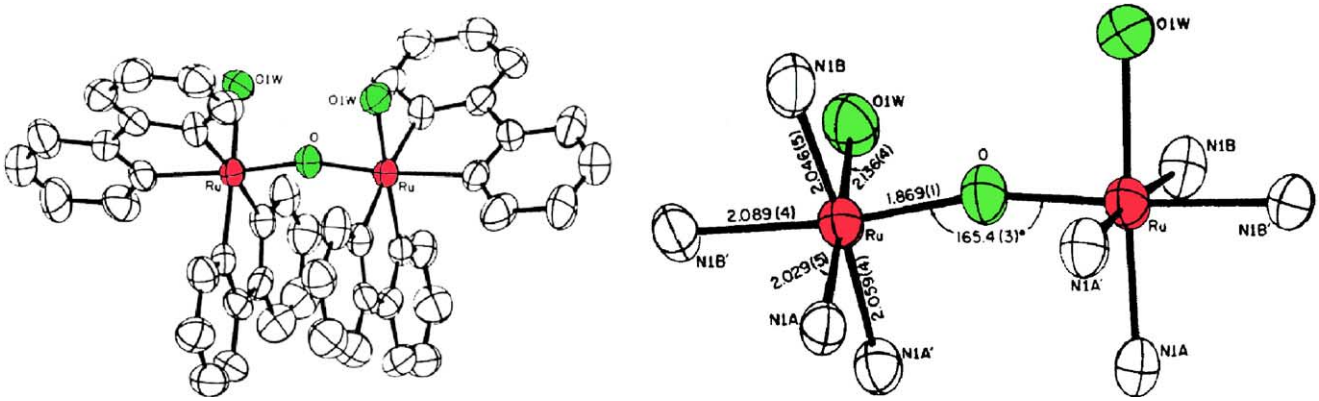

Fig. 2. Crystallographic structures of {3,3}. The left panel shows the complete ligand set for the cation; the right panel shows only the metals and coordinating atoms (adapted from [38]).

modes are mixed, the normal coordinate vibration includes motion of the O atom, and the vibrational frequency depends upon its mass. Larger angles engender greater mixing and larger mass-dependent frequency shifts. By measuring the isotope-induced frequency shifts, one can calculate the bonding angles from the secular equations describing these motions [61]. For the {3,3} ions, $[(bpy)_2Ru(OH_2)]_2O^{4+}$ and $[(bpy)_2(OH_2)RuORu(OH)(bpy)_2]^{3+}$, shifts of 2–3 cm^{-1} were measured upon substitution of ^{18}O in the bridge, corresponding to calculated Ru–O–Ru bridging angles of 166–169° [46,59]. Thus, it appears that the solid and solution structures are very similar. This method can also be used to assess the bridging angle in the {4,4} and {5,5} higher oxidation states (succeeding paragraphs), for which crystal structures are not available. From ^{18}O-induced shifts in ν_s of −2 and −5 cm^{-1}, the calculated angles are 168° for {4,4} and 162° for {5,5} (H. Yamada, unpublished observations) [62].

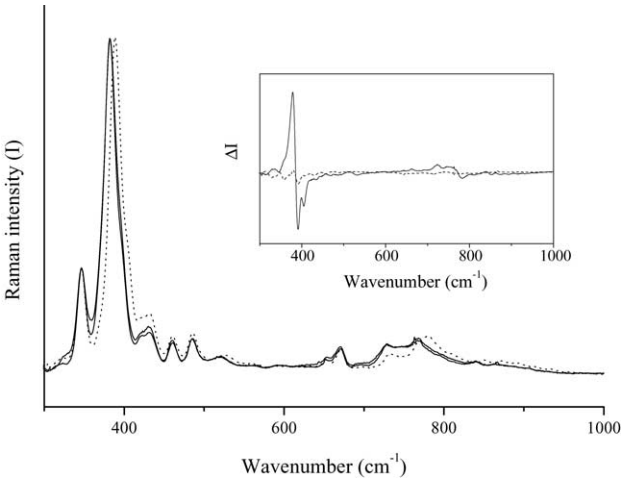

Fig. 3. Normalized RR spectra of {3,4} at 488 nm excitation containing ^{16}O (dashed line) or ^{18}O in the μ-oxo bridging position. The inset shows the ^{18}O—^{16}O difference spectrum (solid line) and the difference spectrum for the ^{18}O-substituted complex before and after 10 cycles of the catalyst (dashed line) [59].

These μ-oxo ions display higher oxidation states that are electrochemically accessible in aqueous solution. As emphasized by Meyer and coworkers [38,53,56,63,64], this attribute is a consequence of their possessing coordinated water, which can undergo simultaneous deprotonation with electron loss, thereby avoiding accumulation of high electrostatic charge. The redox properties of these ions have historically been determined by cyclic voltammetry and related electrochemical techniques [38,53,56,63]. Although several technical problems have been cited with the use of these methods, including slow electrode kinetics arising from proton gains or losses accompanying change in redox states [65,66], inherent irreversibilities of the higher oxidations [38,50,52], adsorption [49] and electrode deterioration [53], other standard methods such as spectroelectrochemical titrations are not feasible because the ions in their higher oxidation states are difficult to distinguish by optical spectroscopy and are unstable with respect to their reaction with solvent H_2O.

Using cyclic voltammetry and differential pulse polarography, Meyer and coworkers determined the following oxidation sequence for the $[(bpy)_2Ru(OH_2)]_2O^{4+}$ ion [38]:

$$\{3,3\} \rightarrow \{3,4\} \rightarrow \{4,5\} \rightarrow \{5,5\}$$

where for simplicity, deprotonation of the {3,3} and {3,4} ions has not been indicated. These ions exhibit the following acid-base equilibria:

$$[(bpy)_2Ru(OH_2)]_2O^{n+} \rightleftharpoons$$
$$[(bpy)_2(OH_2)RuORu(OH)(bpy)_2]^{(n-1)+} + H^+ \rightleftharpoons$$
$$[(bpy)_2Ru(OH)]_2O^{(n-2)+} + H^+$$

where n = 4, pK_1 = 5.9, pK_2 = 8.3 for {3,3}, and n = 5, pK_1 = 0.4, pK_2 = 3.3 for {3,4} [38]. From the pH-dependence of the potentials, it was ascertained that the oxidation states {4,5} and {5,5} were both fully deprotonated, i.e., were dimeric ruthenyl ions, $[(bpy)_2Ru(O)]_2O^{n+}$, n = 3, 4, respectively, over the entire investigated pH range (0–13). The inability to detect the {4,4} oxidation state was ascribed to its instability with respect to disproportionation

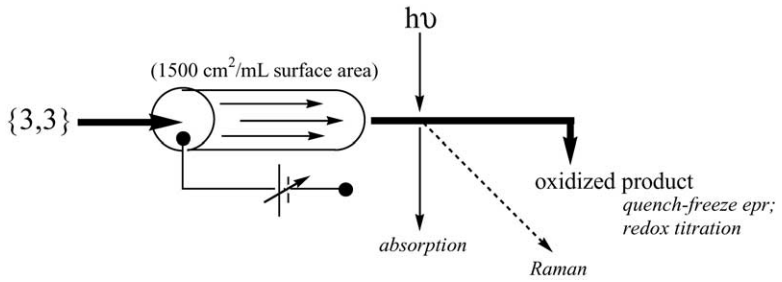

Fig. 4. Flow electrolysis for analysis of higher oxidation states.

[38]. This behavior is surprising—particularly since the similar $[(tpy)Ru(OH_2)_2]_2O^{4+}$ ion has been shown to give a regular progression of increasing reduction potentials with oxidation state through the series $\{3,3\} \rightarrow \{3,4\} \rightarrow \{4,4\} \rightarrow \{4,5\}$ [53]—and its chemical origins have not been identified.

As an alternative approach to determining redox states, we have developed electrochemical methods that utilize a columnar flow-through electrode with high surface area/volume (typically 1500 cm^2/mL) ratios to effect rapid constant potential electrolysis of the solutions. A schematic diagram of the apparatus is given in Fig. 4. In this device, the redox poise of the effluent solution is essentially the value set by the potentiometer; the flowing solutions can be analyzed directly by optical or RR spectroscopy or collected for chemical and physical analyses. The major limitation that we have found in investigating the redox properties of $[(bpy)_2Ru(OH_2)]_2O^{4+}$ by this method is that oxidation is incomplete in solutions that are not highly acidic (pH > 1), which appears to be a consequence of high background electrolysis of water. Results of a typical RR spectroelectrochemical titration of the {3,4} ion [49] are shown in Fig. 5. Upon increasing the potential, the {3,4} spectrum dominated by an intense ν_s band at 389 cm^{-1} decreases with concomitant appearance of an intermediate spectrum whose major feature is a band at 358 cm^{-1}; this band is also assignable to ν_s on the basis of its ^{18}O-isotope dependence. At higher potential, the intermediate disappears in favor of a species with a significantly altered spectrum whose dominant feature is a band at 818 cm^{-1}. This latter band has been identified as the stretching mode of a ruthenyl Ru=O bond ($\nu_{Ru=O}$) formed upon deprotonation of the aqua ligands in the highest oxidation state of the complex [46,49]. This assignment is based upon the following observations: The band position does not shift upon isotopic substitution in the bridge, but does shift to 780 cm^{-1} ($\Delta\nu$ = 38 cm^{-1}) upon substitution of the *cis*-aqua ligands with $H_2{}^{18}O$ [46,67]. This behavior excludes the Ru–O–Ru asymmetric stretching mode, but does not distinguish between the possibilities that the band is the Ru=O stretch or the O–O stretching mode of a bound peroxide. The latter was excluded by performing a mixed-isotope experiment, which revealed only two intense bands in this region, at 780 cm^{-1} ($Ru=^{18}O$) and 818 cm^{-1} ($Ru=^{16}O$); had this mode been a peroxo stretch, a third band would have been observed at ~799 cm^{-1}, the three bands arising from the isotopically distinct ^{18}O–^{18}O, ^{18}O–^{16}O, and ^{16}O–^{16}O species. The redox titrimetric nature of the changes in the RR spectra are clearly illustrated by plotting the relative intensities of the bands versus applied potential (Fig. 5, inset). Qualitatively similar results were previously obtained by using Ce^{4+} as a chemical oxidant [47]; however, in this case, the redox poise of the solutions was not well defined. In any event, the data clearly identify the formation of two species with oxidation states higher than the {3,4} ion.

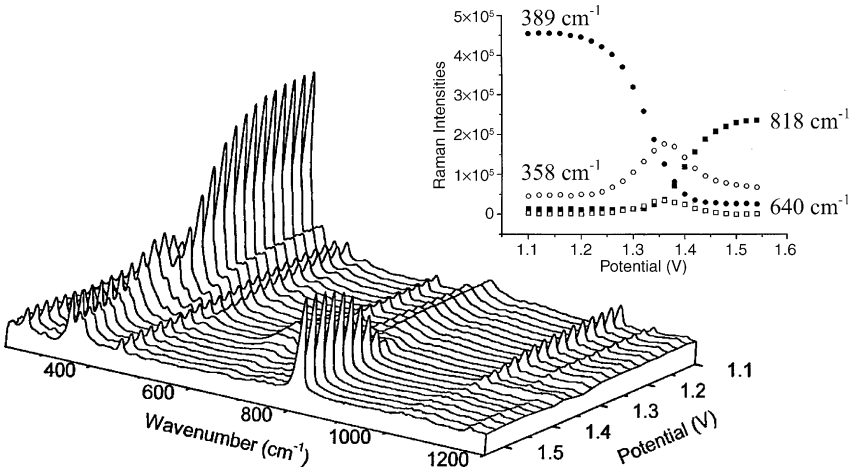

Fig. 5. RR spectroelectrochemical titration of {3,4} [49]. The inset shows the band intensities plotted as a function of the applied potential.

The oxidation state of the most highly oxidized species was determined by reaction of effluent solutions with excess $Os(bpy)_3^{2+}$ (E° = 0.60 V versus Ag/AgCl); this ion will quantitatively reduce the higher oxidation states of the dimer to {3,3}, i.e., the reaction:

$$n\mathrm{Os(bpy)_3}^{2+} + \{\mathrm{Ru_2O^{ox}}\} \rightarrow n\mathrm{Os(bpy)_3}^{3+} + \{3,3\}$$

without forming more reduced species that undergo irreversible decomposition by cleavage of the μ-oxo bridge [38]. In the equation, $\{Ru_2O\}$ represents the summation of species with oxidation states above the {3,3} ion and n is the net oxidizing equivalents accumulated in the flow cell effluent. Plots of spectrophometrically determined values of n versus applied potential clearly show that the most highly oxidized species is 4 equivalents more oxidizing than the {3,3} ion, i.e., the {5,5} ion (Fig. 6, left panel).

The oxidation state of the intermediate was determined by redox titration with Ce^{4+}, following determination of the individual component spectra from spectroelectrochemical titrations identical to those described in Fig. 5, but with optical detection [49]. In strong acid, the {3,4} ion exhibits an asymmetrical visible band with a maximum absorbance at 450 nm and a pronounced shoulder at ~490 nm, representing the two protic forms of the complex, $[(bpy)_2Ru(OH_2)]_2O^{5+}$ and $[(bpy)_2(OH_2)RuOR(OH)(bpy)_2]^{4+}$, respectively, present under these conditions [38]. The intermediate gave a symmetrical band at 488 nm ($\varepsilon_{488} = 1.6 \times 10^4\ M^{-1}\ cm^{-1}$) and {5,5} ion a very similar symmetrical band at 482 nm ($\varepsilon_{482} = 1.5 \times 10^4\ M^{-1}\ cm^{-1}$) [49] that was identical to spectra obtained when the {3,4} ion was reacted with an excess of Ce^{4+}. Addition of one equivalent of Ce^{4+} caused the spectrum of the {3,4} ion to convert quantitatively to that of the intermediate (Fig. 6, right panel) [67]. Thus, the oxidation state of the intermediate species is {4,4} and, at least in triflic (CF_3SO_3H) acid, the oxidation sequence of the *cis,cis*-$[(bpy)_2Ru(OH_2)]_2O^{4+}$ ion is

$$\{3,3\} \rightarrow \{3,4\} \rightarrow \{4,4\} \rightarrow \{5,5\}$$

with the {4,5} ion being thermodynamically unstable [68]. These assignments are also consistent with structural inferences drawn from the RR spectra. Based upon the protic equilibria exhibited by the {3,3} and {3,4} ions, one would anticipate that the {4,4} ion should be predominantly $[(bpy)_2Ru(OH)]_2O^{4+}$ in acidic media, and therefore not display a $\nu_{Ru=O}$ band, whereas, according to the interpretation given the cyclic voltammetric data [38], {4,5} contains terminal ruthenyl groups. The absence of a detectable $\nu_{Ru=O}$ band in the RR intermediate spectrum is therefore consistent with the former assignment, but not the latter [68].

3.2. Identification of the catalytically active oxidation state

Initial rates of O_2 evolution in the presence of excess Ce^{4+} [49] or Co^{3+} [48] are linearly dependent upon the catalyst concentration; from a full steady-state kinetic analysis of the data, it was concluded that the O_2-evolving species must be either the {5,5} ion or a higher oxidation state [48]. This analysis assumes that the rate-limiting step is decomposition of the O_2-evolving species; if so, then the linear dependence indicates that O_2 is obtained from a single catalyst ion. The turnover rate constant (k_{cat}) increases progressively with temperature from 3.7×10^{-3} to $4.5 \times 10^{-2}\ s^{-1}$ in 0.5 M CF_3SO_3H over the range of 10–60 °C, giving as apparent activation parameters $\Delta H^\ddagger = 7.6 \pm 1.2$ kcal/mol and $\Delta S^\ddagger = -43\ (\pm 4)$ cal/deg mol [59]. The solvent deuterium isotope effect (KIE) was 1.7, measured at 23 °C.

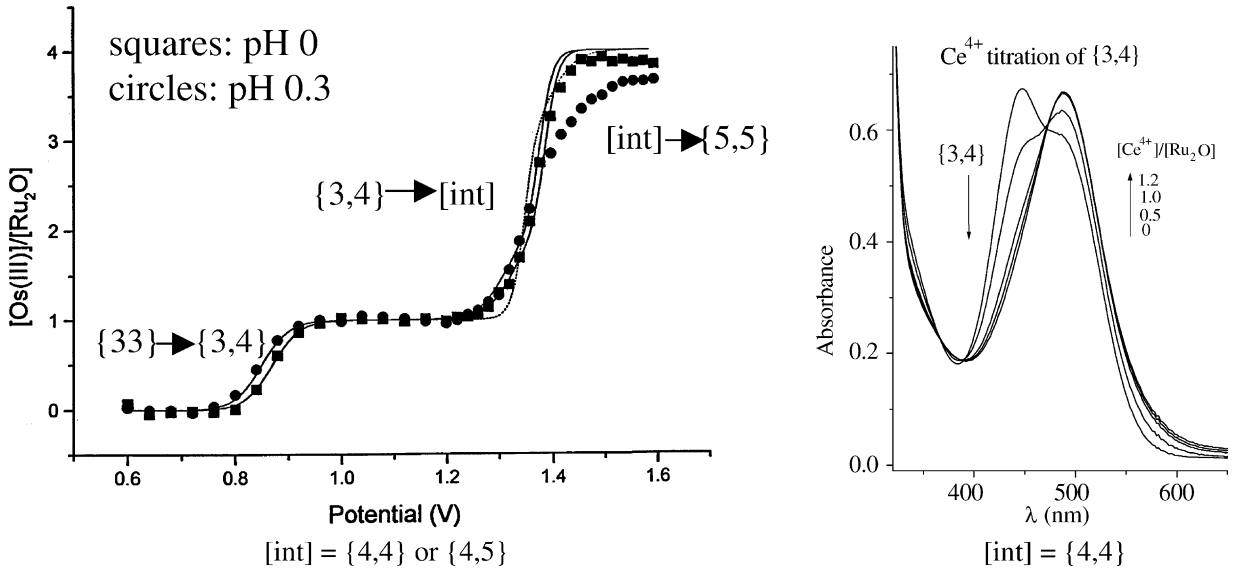

Fig. 6. Left panel: dependence of the stoichiometry of $Os(bpy)_3^{2+}$ oxidation by the μ-oxo ion upon the applied potential at pH 0.3 and pH 1 [49]. Right panel: optical changes accompanying oxidation of {3,4} by Ce^{4+} [67].

The capability of preparing by flow electrolysis essentially pure solutions of the μ-oxo ion in its higher oxidation states allows one to compare quantitatively their decay kinetics to that of O_2 evolution. In triflic acid, electrochemically prepared solutions of {5,5} decay relatively rapidly to the {4,4} ion, which then undergoes ∼10-fold slower decay to the {3,4} state, which is thermodynamically stable [69]. The {5,5} decay is first-order, giving apparent activation parameters in 0.5 M CF_3SO_3H of $\Delta H^{\ddagger} = 7.9$ (± 1.2) kcal/mol and $\Delta S^{\ddagger} = -44$ (± 4) cal/deg mol, and a KIE of 1.6 (23 °C) [59]. The close correspondence of kinetic parameters for O_2 evolution and {5,5} decay, coupled with the much slower decay of the other oxidation states, indicates that only the {5,5} is kinetically competent to be the catalytically active form of the complex. The following reaction scheme, which cannot distinguish between O_2 and H_2O_2 as the immediate oxidation product, is consistent with these data (Scheme 2). However, in this strongly oxidizing environment, H_2O_2 would not accumulate, but be rapidly converted to O_2 following its rate-determining formation.

A different reaction model has been advanced by Meyer and coworkers based primarily upon global kinetic analyses of spectrophotometrically detected reaction transients following oxidation of $[(bpy)_2Ru(OH_2)]_2O^{4+}$ with Ce^{4+} [41,42]. These researchers also conclude that the intermediate ({4,5} in their scheme) decays too slowly to be the active catalyst, and suggest that {5,5} is the reactive form. However, they observed that Ce^{4+} consumption slows dramatically after passage of the μ-oxo ion through several catalytic cycles, and that the onset and extent of this retardation was dependent upon the identity of the acid in the medium. Additional studies demonstrated that this retardation was temporal, suggesting that the catalyst becomes kinetically trapped in an inactive form. The inactive form was suggested to be an anated {3,4} complex formed by competitive substitution of the acid anion over water at vacant coordination sites generated upon oxidation of the *cis*-aqua ligand, e.g., Scheme 3.

In this scheme, because it lacks a second coordinated water, the anated complex cannot be oxidized to the {5,5} state without first undergoing aquation to the diaqua form. Consequently, the unreactive {3,4} ion accumulates and the reaction becomes limited by its aquation rate. Presumably, the very similar optical properties of the diaqua and anated {3,4} ions [42] prevents spectrophotometric determination of the distribution of these species in solution during reaction. Similar unreactive anionic intermediates were also proposed for reactions catalyzed by $[(tpy)Ru(OH_2)_2]_2O^{4+}$ [53] and

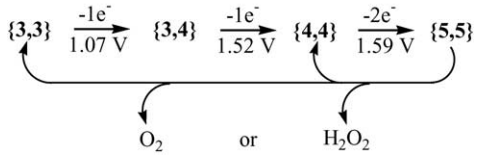

Scheme 2.

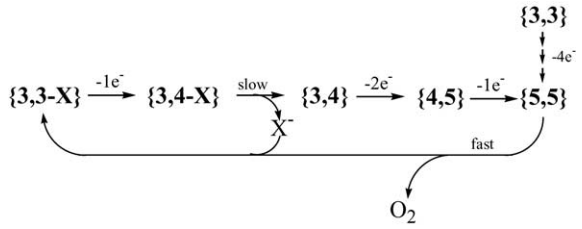

Scheme 3.

$[(bpy)_2(py)RuORu(H_2O)(bpy)_2]^{4+}$ [49], and for catalysis of Cl^- oxidation by the μ-oxo ions [70,71].

Although these reaction models appear dissimilar, they are not necessarily irreconcilable. Strong outer-sphere ion association between $Fe(bpy)_3^{2+}$ and several anions, including ClO_4^-, has been reported [72–74]; as noted in Section 2, this observation has been used to support one proposed mechanism for oxidation of OH^- by $M(bpy)_3^{3+}$ ions [18]. Assuming that the one-electron potentials for {4,4} and {4,5} reduction are very similar, selective ion-pairing of one of the oxidation states (presumably, {4,5}) could reverse the order of thermodynamic stability when the electrolyte contains the associating anion. Thus, the identity of the accumulating intermediate would be medium-dependent, as observed. Furthermore, the presence of associated anions within the second coordination sphere of the complex would promote inner-sphere anation following release of the oxidized aqua ligand to generate inactive forms of the catalyst in the manner envisioned by Meyer. Conversely, we are confident that formation of anated complexes is not extensive when the reactions are run in CF_3SO_3H using our experimental protocols. Anionic substitution at the *cis*-aqua positions causes readily detectable changes in the cyclic voltammograms of the complexes, including large cathodic shifts in the {3, 3} ⇌ {3, 4} midpoint potential and loss of the characteristic catalytic wave for water oxidation [50,52,70]. However, cyclic voltammograms of the effluent {5,5} solutions obtained from the flow electrolysis cell were identical to voltammograms of the reactant {3,3} solutions and underwent no change in structure over an extended period of time [49]. Consequently, the amount of anated complexes formed during electrochemical preparation of the {5,5} ions was below detectable levels.

A second complication evident in ClO_4^--containing solutions is the tendency of the higher oxidation states of the complexes to form precipitates [75]. The precipitate is catalytically active and slowly redissolves with the evolution of O_2 to give final solutions of {3,4} [42,46]. Resonance Raman spectra of the solid gave the same intense bands as recorded for the complex in solution (Fig. 5), indicating that the solid was a μ-oxo dimer that contained the {5,5} ion [42].

3.3. Ligand substitution dynamics

Exchange of the bridging O atom with solvent H_2O in the {3,3} and {3,4} ions is exceptionally slow and is de-

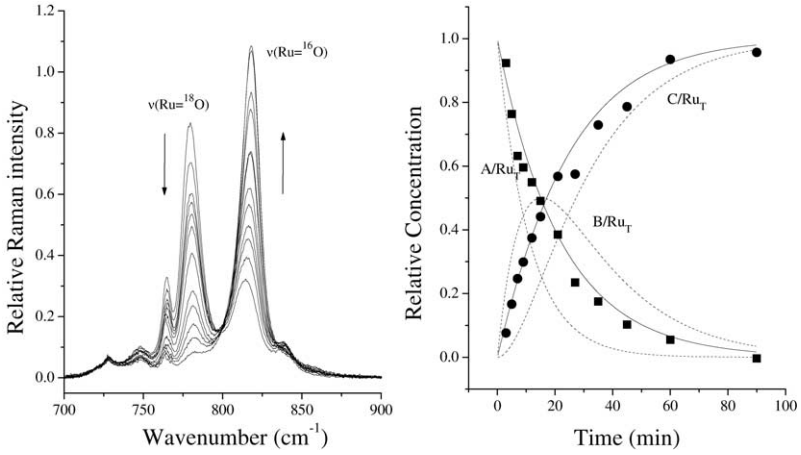

Fig. 7. Time dependence of isotopic change in the {3,3} *cis*-aqua positions [67].

tectable only after heating solutions above 60 °C for several hours [46]. There is no exchange at this position during catalytic turnover (Fig. 3) [46,49,67]. In marked contrast, solvation or anation at the *cis*-aqua positions in the {3,3} is facile [46,76,77]. As originally demonstrated by Meyer and associates [76] by using nmr techniques, substitution of deuteroacetonitrile or Cl^- for H_2O to form the unsymmetrical {3,3} ions, $[(bpy)_2(X)RuORu(OH_2)(bpy)_2]^{n+}$, occurs with $t_{1/2} \leq 10$ min. We have recently measured rate constants for water exchange in the {3,3} and {3,4} ions in triflic acid by RR spectroscopy [67]. The method entails incubating the ^{18}O-labeled complexes in solutions of normal isotopic composition for timed periods, followed by quantitative oxidation with Ce^{4+} ion to the {5,5} state and measuring the relative areas of the Ru=^{18}O and Ru=^{16}O bands at 780 and 816 cm^{-1}, respectively (Fig. 7, left panel).Changes in relative intensities fit the familiar A → B → C rate law for exchange, i.e., (Scheme 4) (Fig. 7, right panel), from which a first-order exchange rate constant for {3,3} of $k_{\{3,3\}} = 7 \times 10^{-3}\ s^{-1}$ (23 °C), was determined. In contrast, no exchange was observed within 3 h in the {3,4} ion, setting an upper limit for exchange in this oxidation state of $k_{\{3,4\}} \leq 10^{-5}\ s^{-1}$ (23 °C).

The rate constant for exchange at the *cis*-aqua positions in the {3,3} ion is 10^3–10^5-fold greater than rate constants measured for anation of monomeric $(bpy)_2Ru^{III}X(H_2O)^{3+}$ ions bearing simple σ-donor ligands (X). As discussed in detail elsewhere [67], there are several potential factors that may contribute to this dramatic rate enhancement. First, comparison of redox potentials and acidities of aqua ligands in the μ-oxo ions with those of monomeric analogs indicate that coordination of the $ORu(OH_2)(bpy)_2^+$ unit effectively increases the electronic charge on the Ru(III) center [54,66]. For monomeric Ru(II) tetraammine and bis-bipyridine complexes with the general formulas $Ru(NH_3)_4X(OH_2)^{n+}$ and $Ru(bpy)_2X(OH_2)^{n+}$, anation rates are strongly accelerated when the fifth nonexchangeable ligand (X) is strongly σ-donating [78–82]. Second, the Ru–O–Ru symmetric stretching mode in the {3,3} ion shifts slightly to lower energies ($\Delta\nu_s \simeq 2\ cm^{-1}$) in D_2O [46,59], an effect which we have attributed to H-bonding of solvent to the bridging μ-oxo atom. Similar shifts have been observed in Fe–O–Fe ν_s modes where H-bonding has been confirmed by X-ray crystallography [83,84]. H-bonding could increase the nucleophilicity of the attacking water and promote reaction by associative pathways [85]. A third potential factor, evident in the crystal structure [38], is the relatively large distortion in the primary coordination sphere away from pseudo-O_h symmetry, which is apparently caused by multiple bonding to the bridging O atom. This distortion may generate a steric "hole" in the coordination sphere, facilitating approach of the incoming ligand. Similar arguments have been advanced to account for the anomalously rapid substitution at the aqua position in the $Ru^{III}(edta)(OH_2)^-$ ion [86-88].

3.4. Formation of the O–O bond

Several different pathways have been considered for formation of the covalent O–O bond; a representative (but not exhaustive) set is given in Fig. 8. This set includes both pathways involving unimolecular reductive elimination of the *cis*-ruthenyl oxo atoms from {5,5}, giving directly O_2 and {3,3} or, alternatively, H_2O_2 and {4,4}, and path-

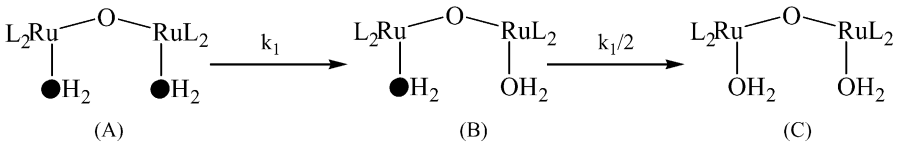

Scheme 4.

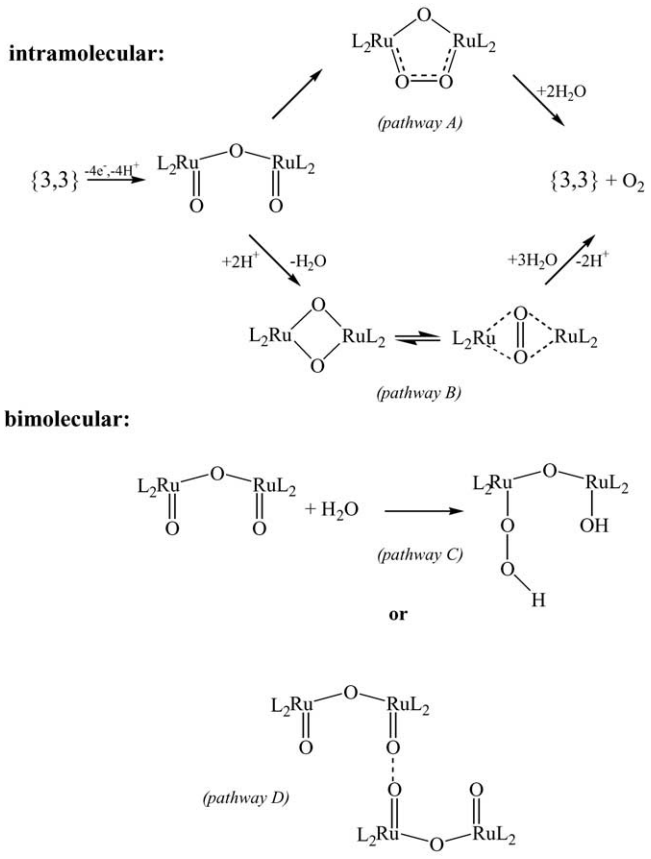

Fig. 8. Alternative hypothetical pathways for water oxidation.

ways involving bimolecular reaction between either two catalyst ions or a catalyst ion and solvent to form peroxo intermediates. Pathway B, which features formation of a symmetric dibridged intermediate that transforms into a μ-η^2-η^2-O_2 bound species, has precedent in the chemistry of di-μ-oxo copper complexes [89]. It can be eliminated from consideration for catalysis by the dimeric ruthenium ions, however, because substitution at the bridging position does not occur during catalyst turnover (Fig. 3). The plausibility of pathway A, in which a mixed dibridged μ-oxo-μ-1,2-peroxo intermediate is proposed, has been questioned on the basis of the large internuclear equilibrium separation between the *cis*-aqua oxygen atoms noted in the crystallographic and RR studies. One study directed to this point made use of complexes in which one of the bipyridines on each ruthenium was bridged by a *n*-alkyl chain attached to the 5-positions [45]. Molecular modeling studies indicated that the large O···O separation distance between the aqua ligands was maintained in the derivatized {3,3} complexes and that small deviations from the energy-minimized structure caused large increases in the internal energy of the molecule such that formation of the dibridged species as a reaction intermediate was not energetically feasible, i.e., the alkyl bridge between adjacent bipyridine ligands effectively "locked-in" the equilibrium conformation. Despite this structural rigidity, the derivatized complex exhibited electrochemical properties, including accumulation of O_2 during electrolysis, that suggested that the catalytic activities of the derivatives were actually superior to that of the underivatized $[(bpy)_2Ru(OH_2)]_2O^{4+}$ ion, from which Petach and Elliott concluded that O_2 could not be formed by unimolecular reductive elimination reactions such as illustrated in pathway A [45].

The relative contributions of these types of pathways has also been determined by ^{18}O-isotope labeling experiments [40,46,59]. Selective labeling of the *cis*-aqua and bridging positions is straightforward, given the markedly different substitution rates at these positions in the {3,3} ion and the very slow exchange rates in the {3,4} ion. However, quantitative differences, most likely caused by the inability to achieve single-turnover conditions, existed in the measured distribution of O_2 isomers from early studies that relied upon periodic sampling of accumulated gases [40,46]; these differences rendered equivocal some of the mechanistic conclusions [42]. To address this problem, we have recently developed mass spectrometric-based techniques that allow real time analysis of the evolved O_2 and other gases that might be formed in side reactions [59]. A schematic diagram of the apparatus used is given in the left panel in Fig. 9; the corresponding distribution of O_2 isotopes following addition of excess Ce^{4+} plotted as a function of time is shown in the right panel for a solution whose composition is ~90% $[(bpy)_2Ru(=^{18}O)]_2{}^{16}O^{4+}$ in ~8% $H_2{}^{18}O$ [90]. This reaction has the following characteristics: nearly equimolar $^{34}O_2$ and $^{32}O_2$, but very little $^{36}O_2$, is formed. The rate of formation of $^{32}O_2$ slowly increases relative to $^{34}O_2$ as the reaction proceeds, consistent with isotopic dilution at the *cis*-aqua positions attending incorporation of coordinated $H_2{}^{18}O$ in the $^{34}O_2$ product. The absence of large changes in isotope distributions with time also indicates that exchange between the {5,5} ruthenyl O atoms and solvent H_2O is slow relative to the rate of O_2 formation, i.e., that isotopic scrambling does not occur. Control experiments made in the absence of added {3,4} gave no increase in O_2 background levels; furthermore, background levels of N_2 (*m/z* = 28 amu) did not change during reaction. Taken together, these controls indicate that all of the O_2 formed following Ce^{4+} addition was from the catalyzed reaction. Furthermore, in contrast to the reactions of $Ru(bpy)_3{}^{3+}$ with OH^- [16], only traces of CO_2 (*m/z* = 44 amu) were detected over the course of the reaction. By this criterion, the μ-oxo ion is considerably more stable to oxidative degradation than is the monomeric ion.

Analyses of the isotopic distribution data indicate that pathways involving unimolecular elimination of O_2 (pathways A and B) or bimolecular reactions between two catalyst ions (pathway D) do not contribute measurably to O_2 formation [91], but that O_2 formation likely arises from two pathways involving (1) reaction between one terminal ruthenyl O and solvent H_2O (pathway C) and (2) a reaction in which both O atoms are derived from solvent [92]. This conclusion was also reached earlier, albeit with less precise data, from isotopic distributions of O_2 formed in {5,5}-catalyzed water oxidation by Co^{3+} [46]. The relative contribution of the path-

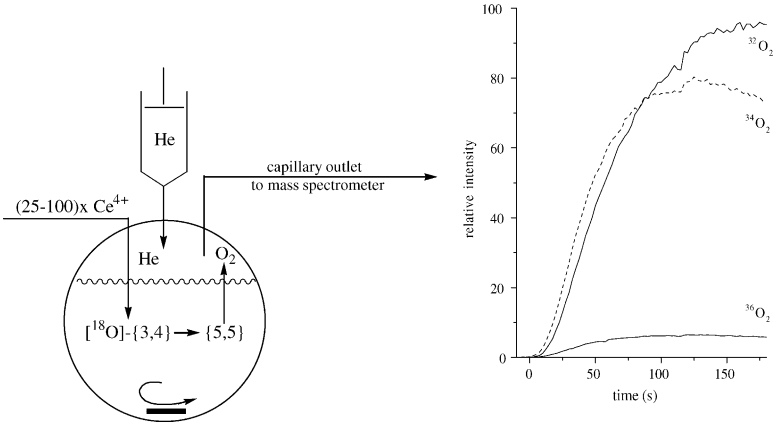

Fig. 9. Apparatus for measuring O_2 isotopic distribution and a typical result [59].

way involving oxidation of two solvent molecules increased with temperature, indicating a slightly higher activation enthalpy ($\Delta\Delta H^{\ddagger} \simeq 5$ kcal/mol); the relative contributions of the two pathways was insensitive to deuteration of the solvent and, within experimental uncertainty, independent of catalyst concentration over the range [{5,5}] = 0.04–0.8 mM [58].

3.5. Reactive intermediates and molecular mechanisms

A plausible mechanism for the pathway in which one O atom is derived from solvent and the other from a coordinated ruthenyl group is shown in Scheme 5.

In this scheme, the elements of H_2O are added across the two ruthenyl groups to form a hydroperoxy intermediate that undergoes following oxidation reactions to ultimately give O_2. The mechanism may be formally analogous to oxidations of O–H and C–H bonds in a wide variety of compounds by monomeric ruthenium polypyridyl compounds (e.g., $[(bpy)_2(py)Ru^{IV}O]^{2+}$) [93–97] in the sense that it could be initiated by H-atom abstraction from solvent. If so, then this reaction must be coupled to peroxo bond formation at the other ruthenyl center because formation of free $OH^{\bullet}$ is energetically prohibitive, i.e., $\Delta E^{\circ} \leq -1.3$ V for the reaction, $\{5,5\} + H_2O \rightarrow \{4,5\} + OH^{\bullet}$ [59]. In contrast, the two-electron oxidation process implicit in the concerted reaction is probably only slightly energonic (cf., $\{5,5\} + 2H_2O \rightarrow \{4,4\} + H_2O_2$, for which $\Delta E^{\circ} = -0.19$ V [49]). Hydrogen bonding to the bridging O atom may also facilitate this reaction by allowing efficient coupling of the reactions at the two ruthenyl centers. Thus, the requirement for all structural

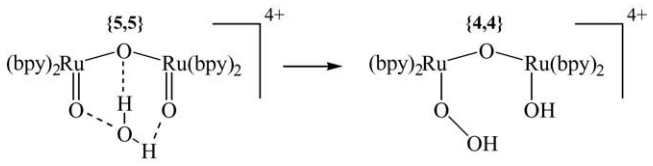

Scheme 5.

elements of the Ru(=O)ORu(=O) center for efficient catalysis can be adequately rationalized. Templating of the reactive H_2O within this site may also provide an explanation why the solvent deuterium KIE is much less than generally observed in H-atom abstraction reactions of monomeric ruthenyl complexes [93,94,98].

The other pathway, in which both O atoms in O_2 are derived from solvent, is more problematic. However, some insight may be derived from the properties of reactive transients detected during catalytic turnover. The {3,3} ion is weakly paramagnetic at room temperature [57,76], but shows no cryogenic epr signal, consistent with spin delocalization over the Ru–O–Ru unit to give a singlet ground state [47,57]. One-electron oxidation to {3,4}, either electrochemically or with Ce^{4+}, gives a broad rhombic signal centered at $g \sim 1.8$ in the cryogenic epr spectra, consistent with a $S = 1/2$ spin state (Fig. 10) [47,49]. Upon further oxidation, this signal appears to give way to a second, very similar signal at potentials corresponding roughly to the formation of the {4,4} ion [99]. When oxidized to the {5,5} state, a much sharper, axially symmetric signal is observed in the $g = 2$ region. All of these low-temperature signals diminish in intensity with increasing temperature and are not detectable above ~100 K, indicating that they are attributable to ruthenium complexes.

The axial signal appearing in the most highly oxidized samples is unexpected, since {5,5} is either even-spin or diamagnetic, and should therefore be epr-silent. The species giving rise to this signal appears to comprise <10% of the ruthenium complexes present, based upon comparison of spin densities determined from double integration of this signal with that from an equimolar solution of the {3,4} ion. Its relative intensity is proportional to the {5,5} concentration, and a 6-line set of weak hyperfine interactions ($A \simeq 40$ G) is observed on the $g_{\perp}$ component of the signal (Fig. 10). These characteristics, including the $g \sim 2$ axial symmetry, suggest that the signal is due to a ligand radical, with the hyperfine spectra arising from interactions with single ^{99}Ru or ^{101}Ru nuclei ($I = 5/2$, relative abundance 13 and 17%). This species could be a coordinated bipyridine π-cation radical which

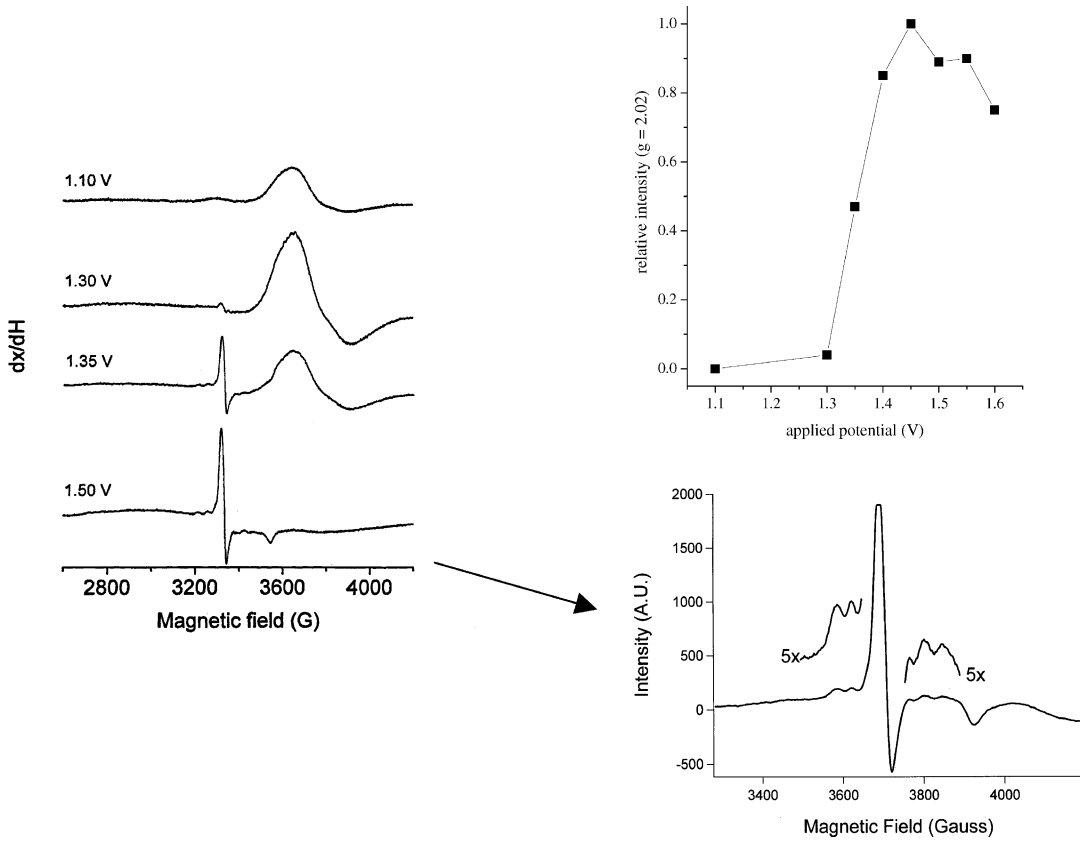

Fig. 10. Cryogenic epr spectra of the μ-oxo ion as a function of applied potential [47,59].

is in equilibrium with {5,5}, i.e., $[(bpy)_2Ru(=O)]_2O^{4+} \rightleftharpoons [(bpy)_2Ru^{V}(=O)ORu^{IV}(=O)(bpy)(bpy_{\pi}{}^{\bullet+})]^{4+}$ or, alternatively, a ligand-based radical formed upon covalent hydration or pseudo-base addition of OH^- to one of the bipyridine ligands. This latter suggestion follows from an earlier mechanistic proposal by Ledney and Dutta, which was based upon the appearance of similar low-temperature epr signals during decomposition of zeolite-entrapped $Ru(bpy)_3{}^{3+}$ [35]. However, the available data do not allow one to identify the radical structures.

Formation of a covalent hydrate might be promoted by H-atom abstraction at a Ru=O center in a concerted reaction similar to that proposed for the other pathway (preceding scheme). In this case, however, the OH segment is positioned to add to the ring 6-position to form a {4,5} intermediate containing a neutral ligand radical, e.g., as suggested in Scheme 6 [100]. This reaction has parallels with the mechanisms proposed for OH^- oxidation by $M(bpy)_3{}^{3+}$ ions discussed in Section 2 that were based upon formation of similar ring-modified intermediates [10-12,16,35]. The presence of a second Ru(V) center in the form of a pendant $[(bpy)_2Ru(=O)O]^+$ moiety may also promote reactivity by functioning as an electron sink for the unpaired electron, facilitating addition of a second solvent molecule to the complex to form a {4,4}-dihydroxy adduct. A similar reaction, albeit bimolecular, has been proposed between $Ru(bpy)_3{}^{3+}$ and the $Ru(bpy)_2(bpy\text{-}OH)^{2+}$ pseudo-base in the overall reaction with OH^- leading to ligand decomposition [16]. Internal ligand-to-metal electron transfer could be fairly slow, as has been demonstrated for the $[Co^{III}(NH_3)_5bpy\text{-}OH^{\bullet}]^{3+}$ radical adduct [103], allowing accumulation of the ligand radical intermediate to epr-detectable levels during catalyst turnover. Unlike $Ru^{II}(bpy)_2(bpy(OH)_2)^{2+}$, the dihydroxy-substituted

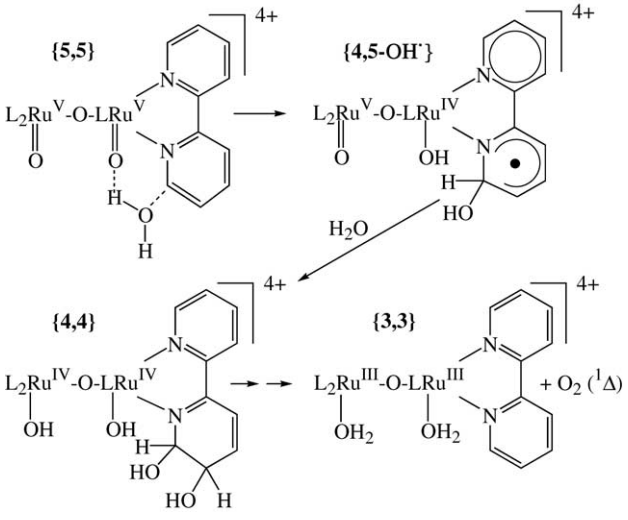

Scheme 6.

ligand in the dinuclear ion is coordinated to a 2-electron oxidizing center which is nearly as strongly oxidizing as the original {5,5} ion. Additional internal electron transfer could drive oxidation of the OH substituents to form, e.g., an unstable endoperoxide that undergoes further bond rearrangement [104] to give O_2 and the {3,3} ion.

Alternative mechanisms proposed to account for this pathway have involved reaction between solvent H_2O with intermediates that contain ruthenium-bound hydroperoxides [46] or 1,3-bridging ozonide (O_3^{2-}) ligands [105]. Although these mechanisms also assign essential roles to both ruthenyl groups, the absence of any chemical precedents for formation of the central intermediates makes them conceptually less appealing. Specifically, as discussed in [59], there appears to be no low-energy pathway for formation of O_2 with both atoms derived from solvent from these species. Reaction by this pathway might also involve expansion of a Ru(V) coordination sphere by addition of H_2O, which then undergoes subsequent reaction with a second solvent molecule. Some support for this notion is obtained from the kinetics of water exchange on monomeric Ru(III) centers, which suggest that an associative interchange mechanism is operative [85], and discussions that encompass a wider chemical literature of 7-coordinate species as potential alternative reaction intermediates to pseudobases and covalent hydrates [28]. However, if this mechanism were operative, one might expect that the intermediate would also provide a pathway for facile exchange of the *cis*-ruthenyl oxygen atoms in {5,5}with solvent H_2O, which is not observed. Furthermore, it is difficult to rationalize by this type of mechanism why the monomeric analog, *cis*-$(bpy)_2Ru(OH_2)_2^{2+}$, as well as dinuclear ions that contain only a single coordinated water such as $[(bpy)_2(py)RuORu(H_2O)(bpy)_2]^{4+}$, are incapable of catalyzing water oxidation. In any event, further characterization of detectable intermediates appearing in the reactions of the $[(bpy)_2Ru(=O)]_2O^{4+}$ ion and its congeners can be expected to provide valuable insights into the underlying water oxidation mechanisms.

4. Reactions of structurally-related μ-oxo ions

There has been considerable interest expressed in evaluating the influence of electron-donating and electron-withdrawing bipyridine ring substituents upon catalytic efficiencies [38,49-52]. In 0.5–1.0 M CF_3SO_3H, the $E_{1/2}$ values measured versus NHE for the {3,3} → {3,4} oxidation step in *cis,cis*-$[L_2Ru(OH_2)]_2O^{4+}$ increases with increasing electron withdrawing character of the substituent, specifically, in the order: 0.90, 1.07, 1.15, and 1.22 V for the ligands: 4,4′-dimethyl-2,2′-bipyridine (DMB) (H. Yamada, unpublished observations), 2,2′-bipyridine [33,44], 2,2′-bipyridyl-4,4′-dicarboxylate (4,4′-CO_2-bpy) [52], and 2,2′-bipyridyl-5,5′-dicarboxylate (5,5′-CO_2-bpy) [50]. This general trend, leading to a difference of ∼300 mV in the apparent one-electron reduction potentials through the series, is consistent with expectations based upon progressive withdrawal of electronic charge from the Ru centers. The anticipated order is inverted for 4,4′-CO_2-bpy and 5,5′-CO_2-bpy, however, which might be due to differing extents of protonation of the pendant carboxyl groups in the two complexes since the carboxylic acid is more strongly withdrawing than is the anion. Consistent with this observation, preliminary estimates place the $E_{1/2}$ value for analogous 5,5′-carbethoxy-2,2′-bipyridine complexes at 1.50 V versus NHE (H. Yamada, unpublished observations), implying that the carboxylate groups in the 4,4′-CO_2-bpy and 5,5′-CO_2-bpy complexes are extensively deprotonated in aqueous CF_3SO_3H.

Based primarily upon their electrocatalytic behavior, the 4,4′-CO_2-bpy and 5,5′-CO_2-bpy derivatives have been suggested by Grätzel and coworkers to much more reactive than the underivatized dimer [50–52]. Both these derivatives have been shown to catalyze water oxidation by Co^{3+} and to catalyze photosensitized water oxidation by tris-RuL^{3+} ions in the presence of sacrificial electron acceptors. The molecular bases for these effects have not been determined, but presumably relate to the greater reaction driving force for water oxidation in the derivatized compounds. In contrast, water oxidation by the DMB complex occurs at a rate that is comparable or even slightly greater than the $[(bpy)_2Ru(OH_2)]_2O^{4+}$ ion. Flow electrochemical/RR spectroelectrochemical analysis of $[(DMB)_2Ru(OH_2)]_2O^{4+}$ has given results very nearly identical to that illustrated in Fig. 5 for $[(bpy)_2Ru(OH_2)]_2O^{4+}$, with the exception that the corresponding reduction potentials are slightly lower (H. Yamada, unpublished observations). Specifically the measured potentials for {3,3} → {3,4}, {3,4} → {4,4}, and {4,4} → {4,5} are 0.94, 1.46, and 1.55 V (versus NHE) for $[(DMB)_2Ru(OH_2)]_2O^{4+}$, compared to 1.07, 1.53, and 1.59 V for $[(bpy)_2Ru(OH_2)]_2O^{4+}$. One notes that the difference between the potentials for the two complexes decreases as the ruthenium formal oxidation state increases, and is only ∼40 mV for the {5,5} ions. Not surprisingly, then, the corresponding decomposition rate constants, measured either by disappearance of the 818 cm^{-1} band in the RR spectra or by absorbance changes accompanying the {5,5} → {4,4} decay, were nearly identical for the two complexes, as were the turnover rate constants measured for O_2 formation from initial rate determinations [49]. Based upon this very limited data set, it appears that catalytic efficiencies in homogeneous reactions may not be very sensitive to substituents present on the bipyridine ligands. Given the apparent existence of two distinct pathways for O_2 formation from the ^{18}O-isotope labeling studies, any realistic mechanistic analysis would require separate analysis of the effects of ring substitution on the isotopic distribution of O_2.

Brudvig and coworkers have recently described the synthesis of a di-μ-oxo-bridged dimanganese complex ($[H_2O(tpy)Mn(O)_2Mn(tpy)OH_2]^{3+}$) that also catalyzes O_2 formation from aqueous solutions of strong oxidants [106,107]. Unlike the monobridged dimeric ruthenium cata-

lysts, the meridianally-bound terpyridine ligands constrain binding of coordinated water to sites that are each *trans* to one of the bridging O atoms, effectively precluding intramolecular elimination reactions as pathways for O_2 evolution (Fig. 9). Turnover rate constants were determined from measured initial rates of O_2 formation to be k_{cat} = 0.7 s^{-1} for oxidation by the peroxomonosulfate anion (oxone, SO_5^-) and $k_{cat} = 2 \times 10^{-3}\,s^{-1}$ for oxidation by the hypochlorite anion (OCl^-) [107]; these values are comparable to the turnover rate constants determined for $[(bpy)_2Ru(OH_2)]_2O^{4+}$-catalyzed oxidation by Ce^{4+} in 0.5 M CF_3SO_3H ($k_{cat} = 1 \times 10^{-2}\,s^{-1}$) [44]. Although attempts to identify the source of O atoms in the reaction using OCl^- as oxidant [103] were confounded by its rapid exchange with solvent $H_2{}^{18}O$ [107,108], it was established in the reaction with oxone that at least some of the O_2 formed occurred by oxidation of water [107]. A reaction mechanism similar to Scheme 5 was proposed for this pathway, i.e., involving formation of a {4,5} dinuclear intermediate containing an Mn=O intermediate which subsequently reacts with solvent H_2O [107].

Acknowledgements

The author is grateful for the dedicated efforts of the graduate students, research associates, and colleagues that have contributed to our research activites in this area, most notably Professor Hiroshi Yamada (National Defense Academy, Tokyo) who, among his many contributions, developed the electrochemical methods for preparing the {5,5} ion that are central to our current investigations, as well as Professors Pierre Moënne-Loccoz, Thomas M. Loehr, and Joann Sanders-Loehr at the Oregon Health & Science University for helpful discussions and making available to us their laser Raman facility, and Professor Thomas J. Meyer (Los Alamos National Laboratory) for technical advice and providing us with compounds synthesized in his laboratory. This work is supported financially by the Division of Chemical Sciences, Office of Basic Energy Sciences, U.S. Department of Energy, under Grant DE-FG03-99ER14943.

References

[1] K.N. Ferreira, T.M. Iverson, K. Maghlaoui, J. Barber, S. Iwata, Science 303 (2004) 1831 (and references cited therein).
[2] C.W. Hoganson, G.T. Babcock, Science 277 (1997) 1953.
[3] V.L. Pecoraro, M.J. Baldwin, M.T. Caudle, H. Wen-Yuan, N.A. Law, Pure Appl. Chem. 70 (1998) 925.
[4] F. Blau, Monatsch 19 (1898) 647.
[5] W.W. Brandt, F.P. Dwyer, E.C. Gyarfas, Chem. Rev. 54 (1954) 959.
[6] F.P. Dwyer, E.C. Gyarfas, J. Am. Chem. Soc. 73 (1951) 2322.
[7] M. Anbar, I. Pecht, Trans. Faraday Soc. 4 (1968) 744.
[8] A.A. Green, J.O. Edwards, P. Jones, Inorg. Chem. 5 (1966) 1858.
[9] G. Nord, O. Wernberg, J.C.S. Dalton, J. Am. Chem. Soc. (1972) 866.
[10] G. Nord, O. Wernberg, J.C.S. Dalton, J. Am. Chem. Soc. (1975) 845.
[11] C. Creutz, N. Sutin, Proc. Natl. Acad. Sci. U.S.A. 72 (1975) 2858.
[12] V.Ya. Shafirovich, A.P. Moravskii, T.S. Dzhabiev, A.E. Shilov, Kinet. Catal. (Eng. Trans.) 18 (1977) 427.
[13] G.M. Malik, G.S. Lawrence, Inorg. Chim. Acta 28 (1978) 149.
[14] J.A.A. Sagüés, R.D. Gillard, R.J. Lancashire, P.A. Williams, J.C.S. Dalton, J. Am. Chem. Soc. (1979) 193.
[15] R.D. Gillard, Coord. Chem. Rev. 16 (1975) 67.
[16] P.K. Ghosh, B.S. Brunschwig, M. Chou, C. Creutz, N. Sutin, J. Am. Chem. Soc. 106 (1984) 4722.
[17] G. Nord, B. Pedersen, E. Bjerbakke, J. Am. Chem. Soc. 105 (1983) 1913.
[18] N. Serpone, F. Bolletta, Inorg. Chim. Acta 75 (1983) 189.
[19] P.A. Lay, W.H.F. Sasse, Inorg. Chem. 24 (1985) 4707.
[20] M. Simić, M. Ebert, Int. J. Rad. Phys. Chem. 3 (1971) 259.
[21] E.S. Floryan, P. Pagsberg, Int. J. Rad. Phys. Chem. 8 (1976) 425.
[22] N.M. Dimitrijević, O.I. Mićić, J.C.S. Dalton, J. Am. Chem. Soc. (1982) 1953.
[23] K.L. Rollick, J.K. Kochi, J. Org. Chem. 47 (1982) 435.
[24] C. Berg-Brennan, P. Subramanian, M. Absi, C. Stern, J.T. Hupp, Inorg. Chem. 35 (1996) 3719.
[25] H-T. Zhang, S.G. Yan, P. Subramanian, L.M. Skeens-Jones, C. Stern, J.T. Hupp, J. Electroanal. Chem. 414 (1996) 23.
[26] J.W. Bunting, Adv. Heterocycl. Chem. 25 (1979) 1.
[27] J.A.A. Sagüés, R.D. Gillard, R.J. Lancashire, P.A. Williams, J.C.S. Dalton, J. Am. Chem. Soc. (1979) 193.
[28] N. Serpone, G. Ponterini, M.A. Jamieson, F. Bolletta, M. Maestra, Coord. Chem. Rev. 50 (1983) 209.
[29] V.Ya. Shafirovich, N.K. Khannov, V.V. Strelets, Nouv. J. Chim. 4 (1980) 81.
[30] J-M. Lehn, J-P. Sauvage, R. Ziessel, Nouv. J. Chim. 3 (1979) 423.
[31] K. Kalyanasundaram, M. Grätzel, Angew. Chem. Int. Ed. Engl. 18 (1979) 701.
[32] M. Hara, C.C. Waraksa, J.T. Leans, B.A. Lewis, T.E. Mallouk, J. Phys. Chem. A 104 (2000) 5275.
[33] B.S. Brunschwig, M.H. Chou, C. Creutz, P. Ghosh, N. Sutin, J. Am. Chem. Soc. 105 (1983) 4832.
[34] K. Kalyanasundaram, O.I. Mićić, E. Pramauro, M. Grätzel, Helv. Chim. Acta 62 (1979) 2433 (These researchers report that, in weakly acidic media, $Fe(bpy)_3^{3+}$ was reduced by RuO_2 to a Fe(II) species whose optical spectrum was distinct from that of $Fe(bpy)_3^{2+}$ without any concomitant formation of O_2. Upon subsequent neutralization in the presence of RuO_2, the spectrum reverted to that of $Fe(bpy)_3^{2+}$ with evolution of a stoichiometric equivalence of O_2. This behavior suggests the formation of chemically modified intermediates which can participate in catalyzed water oxidation.).
[35] M. Ledney, P.K. Dutta, J. Am. Chem. Soc. 117 (1995) 7687.
[36] W.H. Quayle, J.H. Lunsford, Inorg. Chem. 21 (1982) 97.
[37] S.W. Gersten, G.J. Samuels, T.J. Meyer, J. Am. Chem. Soc. 104 (1982) 4029.
[38] J.A. Gilbert, D.S. Eggleston, W.A. Murphy Jr., D.A. Geselowitz, S.W. Gersten, D.J. Hodgson, T.J. Meyer, J. Am. Chem. Soc. 107 (1985) 3855.
[39] S.J. Raven, T.J. Meyer, Inorg. Chem. 27 (1988) 4478.
[40] D. Geselowitz, T.J. Meyer, Inorg. Chem. 29 (1990) 3894.
[41] C.W. Chronister, R.A. Binstead, J.F. Ni, T.J. Meyer, Inorg. Chem. 36 (1997) 3814.
[42] R.A. Binstead, C.W. Chronister, J.F. Ni, C.M. Hartshorn, T.J. Meyer, J. Am. Chem. Soc. 122 (2000) 8464.
[43] K. Honda, A.J. Frank, J. Chem. Soc. Chem. Commun. (1984) 1635.
[44] J.P. Collin, J.P. Sauvage, Inorg. Chem. 25 (1986) 135.
[45] H.H. Petach, C.M. Elliott, J. Electrochem. Soc. 139 (1992) 2217.
[46] J.K. Hurst, J. Zhou, Y. Lei, Inorg. Chem. 31 (1992) 1010.
[47] Y. Lei, J.K. Hurst, Inorg. Chem. 33 (1994) 4460.
[48] Y. Lei, J.K. Hurst, Inorg. Chim. Acta 226 (1994) 179.

[49] H. Yamada, J.K. Hurst, J. Am. Chem. Soc. 122 (2000) 5303.
[50] F.P. Rotzinger, S. Munavalli, P. Comte, J.K. Hurst, M. Grätzel, F.-J. Pern, A.J. Frank, J. Am. Chem. Soc. 109 (1987) 6619.
[51] F.P. Rotzinger, S. Munavalli, P. Comte, J.K. Hurst, M. Grätzel, in: H. Yersin, A. Vogler (Eds.), Photochemistry and Photophysics of Coordination Compounds, Springer-Verlag, Berlin, 1987.
[52] P. Comte, M.K. Nazeruddin, F.P. Rotzinger, A.J. Frank, M. Grätzel, J. Mol. Catal. 52 (1989) 63.
[53] E.L. Lebeau, S.A. Adeyemi, T.J. Meyer, Inorg. Chem. 37 (1998) 6476.
[54] P. Doppelt, T.J. Meyer, Inorg. Chem. 26 (1987) 2027.
[55] The activity measured by Doppelt and Meyer was so low that they could not exclude the possibility that it was derived from impurities in the preparation.
[56] D. Geselowitz, W. Kutner, T.J. Meyer, Inorg. Chem. 25 (1986) 2015.
[57] T.R. Weaver, T.J. Meyer, S.A. Adeyemi, G.M. Brown, R.P. Eckland, W.E. Hatfield, E.C. Johnson, R.W. Murray, D. Unterecker, J. Am. Chem. Soc. 97 (1975) 3040.
[58] J.R. Schoonover, J.F. Ni, L. Roecker, P.S. White, T.J. Meyer, Inorg. Chem. 35 (1996) 5885.
[59] H. Yamada, W.F. Siems, T. Koike, J.K. Hurst, J. Am. Chem. Soc. 126 (2004) 9786.
[60] J. Sanders-Loehr, W.D. Wheeler, A.D. Shiemke, B.A. Averill, T.M. Loehr, J. Am. Chem. Soc. 111 (1989) 8084.
[61] R.M. Wing, K.P. Callahan, Inorg. Chem. 8 (1969) 871.
[62] A similar analysis was made for the {3,4} ion, which showed larger μ-^{18}O dependent shifts in ν_s [46]. This cannot be ascribed simply to a larger bending angle, however, because in this oxidation state, the Ru─O lengths in the Ru─O─Ru unit are also unequal [58], i.e., the stretching mode is inherently asymmetric regardless of the bending angle. Consequently, the O atom will also move in this mode when the Ru─O─Ru bond is linear.
[63] T.J. Meyer, J. Electrochem. Soc. 131 (1984).
[64] T.J. Meyer, Inorg. Chem. 42 (2003) 8140.
[65] A.A. Diamantis, W.R. Murphy, T.J. Meyer, Inorg. Chem. 23 (1984) 3230.
[66] G.E. Cabaniss, A.A. Diamantis, W.R. Murphy, R.W. Linton, T.J. Meyer, J. Am. Chem. Soc. 107 (1985) 1845.
[67] H. Yamada, T. Koike, J.K. Hurst, J. Am. Chem. Soc. 123 (2001) 12775.
[68] These oxidation states were confirmed by another experiment in which equimolar solutions of the {3,3} and electrochemically prepared {5,5} ions were mixed to give a solution whose spectrum was that of the intermediate ({4,4}) [49]. Had either the most highly oxidized species not been {5,5} or the intermediate been {4,5}, the product solution would have contained significant amounts of {3,4}, which is readily detectable in the optical spectra.
[69] One should not draw the conclusion that because {4,4} accumulates, it is the immediate product of {5,5} decomposition. If, for example, the decomposition reaction were {5,5} → {3,3} + O_2, {3,3} would be rapidly oxidized in additional steps to {4,4}. In general, because redox cross-reactions between the complexes are rapid relative to decomposition of the {5,5} [41,42], the distribution of oxidation states will reflect the overall redox poise of the solution at any point in time.
[70] C.D. Ellis, J.A. Gilbert, W.R. Murphy Jr., T.J. Meyer, J. Am. Chem. Soc. 105 (1983) 4842.
[71] W.J. Vining, T.J. Meyer, Inorg. Chem. 25 (1986) 2023.
[72] L. Johansson, Chem. Script. 9 (1976) 30.
[73] L. Johansson, Chem. Script. 10 (1976) 72.
[74] G.I. Gromova, A.K. Pyartman, V.E. Mironov, Russ. J. Inorg. Chem. 23 (1978) 1875.
[75] Our initial observation of this phenomenon [46] prompted us to change the medium to CF_3SO_3H. Meyer and coworkers report complex precipitation also occurs under certain circumstances in triflate-containing media [42], although we have never observed this.
[76] J.C. Dobson, B.P. Sullivan, P. Doppelt, T.J. Meyer, Inorg. Chem. 27 (1988) 3863.
[77] R. Arakawa, N. Kubota, T. Fukuo, O. Ishitani, E. Ando, Inorg. Chem. 41 (2002) 3749.
[78] L.R. Allen, P.P. Craft, B. Durham, J. Walsh, Inorg. Chem. 23 (1987) 53.
[79] B.P. Sullivan, D. Conrad, T.J. Meyer, Inorg. Chem. 24 (1985) 3640.
[80] S.S. Isied, H. Taube, Inorg. Chem. 13 (1974) 1545.
[81] S.S. Isied, H. Taube, Inorg. Chem. 25 (1976) 3070.
[82] D.W. Franco, H. Taube, Inorg. Chem. 17 (1978) 571.
[83] A.D. Shiemke, T.J. Loehr, J. Sanders-Loehr, J. Am. Chem. Soc. 108 (1986) 2437.
[84] R.E. Stenkamp, Chem. Rev. 94 (1994) 715.
[85] I. Rappaport, L. Helm, A.E. Merbach, P. Bernhard, A. Lundi, Inorg. Chem. 27 (1988) 873.
[86] T. Matsubara, C. Creutz, Inorg. Chem. 18 (1979) 1956.
[87] H.C. Bajaj, R. van Eldik, Inorg. Chem. 29 (1990) 2855.
[88] H.C. Bajaj, A. Das, R. van Eldik, J. Chem. Soc., Dalton Trans. (1988) 1563.
[89] J.A. Halfen, S. Mahapatra, E.C. Wilkinson, S. Kaderli, V.G. Young Jr., L. Que, A.D. Zuberbühler, W.B. Tolman, Science 271 (1996) 1379.
[90] Selective enrichment in the terminal oxo positions was achieved by incubating the {3,3} ion in $H_2{}^{18}O$, then terminating exchange by oxidizing the sample to {3,4} with Ce^{4+} (Section 3.3). Following dilution into normal isotopic H_2O and purging the system of O_2, reaction was initiated by adding excess Ce^{4+} [59].
[91] The small amount of $^{36}O_2$ appearing in the mass spectra is quantitatively accountable by reaction between $H_2{}^{18}O$ in the solvent with $[(bpy)_2Ru(=^{18}O)]_2{}^{16}O^{4+}$.
[92] A reviewer has suggested a possible alternative mechanism wherein rapid exchange between an intermediate and solvent leads to the appearance of $^{32}O_2$ in the gaseous product. The kinetic profiles obtained (Fig. 9) indicate that this exchange would have to involve an intermediate formed after the rate-limiting step for O_2 evolution. Since the concentration levels of this intermediate would necessarily be very low and exchange at the *cis*-positions in other higher oxidation states of the μ-oxo ion is undetectably slow, this mechanism is not very appealing. It, however, cannot presently be excluded.
[93] J. Gilbert, L. Roecker, T.J. Meyer, Inorg. Chem. 26 (1987) 1126.
[94] R.A. Binstead, M.E. McGuire, A. Dovletoglou, W.K. Seok, L.E. Roecker, T.J. Meyer, J. Am. Chem. Soc. 114 (1992) 173.
[95] J.M. Mayer, Acc. Chem. Res. 31 (1998) 441.
[96] J.R. Bryant, J.M. Mayer, J. Am. Chem. Soc. 125 (2003) 10351.
[97] J.R. Bryant, T. Matsuo, J.M. Mayer, J. Am. Chem. Soc. 43 (2004) 1587.
[98] J.A. Gilbert, S.W. Gersten, T.J. Meyer, J. Am. Chem. Soc. 104 (1982) 6873.
[99] The {4,4} ion is either even-spin or diamagnetic, and would not be expected to give an X-band epr signal. This signal could arise from the {4,5} ion if the one-electron reduction potentials of the {3,4} and {4,4} ions exhibited temperature dependencies that favored {4,4} accumulation at room temperature and {4,5} accumulation at low temperatures.
[100] Attachment of the OH segment at the ring 5-position, which is the preferential site for $OH^•$ adduct formation [101,102], may be precluded for a concerted reaction by the distance between this position and the ruthenyl O atom. If the reaction were stepwise, i.e., involved a {4,5}-radical cation intermediate, nucleophilic attack of OH^- should occur preferentially at the ring 4-position [23-25].
[101] S. Steenken, P. O'Neill, J. Phys. Chem. 82 (1978) 372.
[102] N. Selvarajan, N.V. Raghaven, J. Phys. Chem. 84 (1980) 2548.

[103] M.Z. Hoffman, D.W. Kimmel, M.G. Simic, Inorg. Chem. 18 (1979) 2479.
[104] H.H. Wasserman, J.R. Scheffer, J. Am. Chem. Soc. 89 (1967) 3073.
[105] T.J. Meyer, in: A.E. Martel, D.T. Sawyer (Eds.), Oxygen Complexes and Oxygen Activation by Transition Metals, Plenum Press, New York, 1988.
[106] J. Limburg, J.S. Vrettos, L.M. Liable-Sands, A.R. Rheingold, R.H. Crabtree, G.W. Brudvig, Science 283 (1999) 1524.
[107] J. Limburg, J.S. Vrettos, H. Chen, J.C. dePaula, R.H. Crabtree, G.W. Brudvig, J. Am. Chem. Soc. 123 (2001) 423.
[108] D.W. Johnson, D.W. Margerum, Inorg. Chem. 30 (1991) 4845.